Supporting Information

Is the fenamate group a polymorphophore? Contrasting the crystal energy landscapes of fenamic and tolfenamic acids

Ogaga G. Uzoh[a], Aurora J. Cruz-Cabeza[b] and Sarah L. Price[a*]

[a]Department of Chemistry, University College London, 20 Gordon Street, London WC1H 0AJ, United Kingdom.

[b]Van 't Hoff Institute for Molecular Sciences, University of Amsterdam, Science Park 904, 1098 XH Amsterdam, The Netherlands.

Table of Contents

1. Discussion of the experimental thermodynamic data (Table 1) for tolfenamic acid polymorphs 2

2. The disordered polymorph V of tolfenamic acid. 3

3. Further computational details..... 5

3.1. Dependence of conformational energy on method..... 5

3.2. Consideration of ξ_2 torsion angle 6

3.3. Further details on Crystal Energy Landscape calculations and intermediate results 7

4. Further comparisons of the hypothetical structures of FA on the crystal energy landscape and known form of TA..... 11

5. Comparison with the newly published crystal structures of flufenamic acid 13

1. Discussion of the experimental thermodynamic data (Table 1) for tolfenamic acid polymorphs

There are four papers with evidence for the thermodynamic relationship between forms I and II, which give different conclusions. The enthalpy and temperature of fusion, ΔH_{fus} and T_{fus}, measurements provide a way of classifying polymorphs as either being monotropic or enantiotropic. Surov et al. showed that the yellow form (form II) is more stable than white form (form I)[1] and that both polymorphs have a monotropic relationship because the form with the higher melting temperature, form II, has a higher enthalpy of fusion, ΔH_{fus}, (by enthalpy of fusion rule)[2] as illustrated in Scheme S1(a). However, Mattei and Li[3] measured an endothermic transformation going from II to I with increasing temperature at 141.8 °C, implying an enantiotropic relationship Scheme S1(b). The observation of the transformation in a slurry experiment implies that the thermodynamic transition point is below room temperature. All three sets of measurements[1,3,4] have form II more stable than form I at 0K.

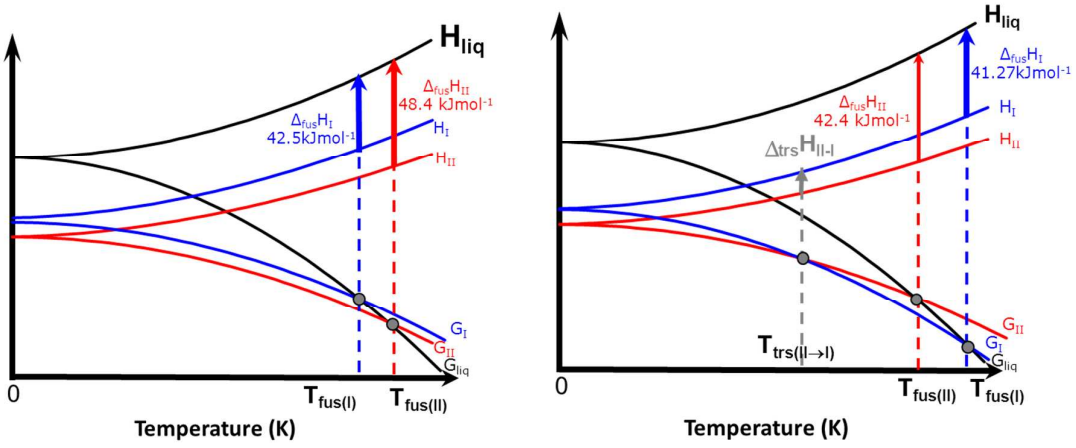

(a) (b)

Scheme S1: Temperature dependence of the enthalpy (H) and free energy (G) diagrams for forms I and II of tolfenamic acid, showing *(a)* monotropic relationship from data from Surov[1], which qualitatively the same as data from Andersen[4] and *(b)* enantiotropic relationship from data from Mattei and Li[3]

Lopez-Mejias et al.[5] provide the only thermodynamic data available for form III – V. They note that heating forms III and V at 80 °C caused a transformation to form I within minutes to hours. In solution, forms III, IV and V transformed to form I or a mixture of form I and II. Hence, form III, IV and V are metastable polymorphs. The heats of fusion given in Lopez-Mejias' supplementary information[5] are listed by the initial form, and forms III and V may well have transformed to form I. Therefore this set of data is inconclusive about the relationship between forms I and II.

2. The disordered polymorph V of tolfenamic acid.

The crystal structure of Form V of TA was solved with an R-factor of 6.58%; the whole molecule is equally disordered over two sites.[5] If we simply separate the two components of disorder, there is a wrong connectivity between the C_8 and N_1 atoms (green in Figure S1b). The C_8-N_1 bond length of 1.70 Å is unusually long and this causes the breakdown of the trigonal planar relationship of nitrogen, C_7-$N_1(H_6)$-C_8 connectivity (Figure S1c).

We can make a model with the two components both corresponding to the expected molecular geometry by redefining the connectivity (Figure S1b) to link half of one disordered molecule (bonded molecule in Figure S1a) and half of the other disordered molecule (atoms only component in Figure S1a) and combining the remaining halves to form the second component. The resulting molecules (red and blue in Figure S1b) now have a C-N bond length of 1.43 Å and a trigonal planar geometry around the nitrogen. We created three ordered Z=2 crystal structures with the unit cell of form V by using the two resulting molecules (Figure S2a, b for $Z'=1$, Figure S2 c for $Z'=2$).

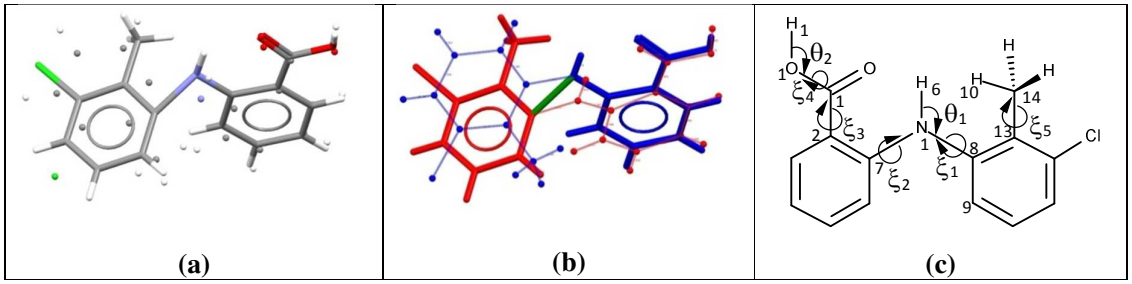

Figure S1: (a) Crystal structure KAXXAI04 of form V of TA (b) The atom connectivity of the two new components (color red and blue); the original C-N connectivity is labeled green (c) Chemical diagram showing the atomic connectivity of TA.

As shown in Table 3, lattice energy minimization of the ordered structures V_a and V_c produces a fairly small change in the cell constants, but the nearest minimum to V_b is rather different, probably because the initial structure contained a close Cl···Cl contact. This structure also corresponds to the most stable of three models of form V. All three structures have a lattice energy that is 6-8 kJmol^{-1} above form I, and so these ordered models of form V are not competitive in energy with the other known polymorphs of TA.

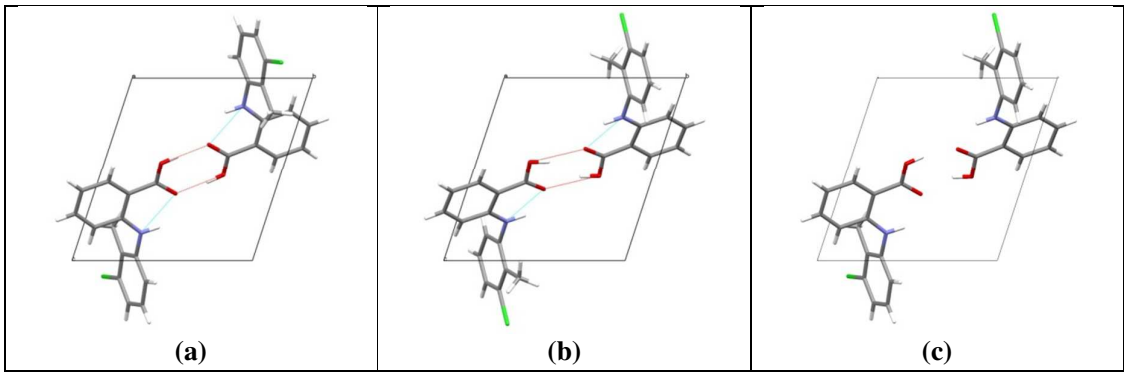

Figure S2: Ordered Z=2 crystal structures formed from the disordered components of TA form V. (a) Form V_a, (b) Form V_b, and (c) Form V_c.

3. Further computational details

3.1. Dependence of conformational energy on method

An appropriate grid of intramolecular energies is essential in order to search all the likely conformations of TA and FA and hence generate all likely Z′=1 crystal structures. All possible values of the ξ_1 torsion angle were scanned[6] at the HF, PBE0, MP2 and B3LYP level of theory allowing the rest of the molecule to relax, using GAUSSIAN[6] to observe the effects that changing the level of theory had on the relative intramolecular energy.

The HF level of theory produced a qualitatively incorrect conformational profile for the ξ_1 torsion angle (Figure S3a). PBE0 is the best compromise because it reproduces the correlation effect present in TA and the minima coincides in the same torsion angle region as that of MP2 and is computationally cheaper than MP2. At PBE0 level of theory, there is a convergence of energy at 6-31+G(d) basis set (Figure S3b). Therefore PBE0/6-31+G(d) was chosen as the appropriate level of theory for the CrystalOptimiser calculations.

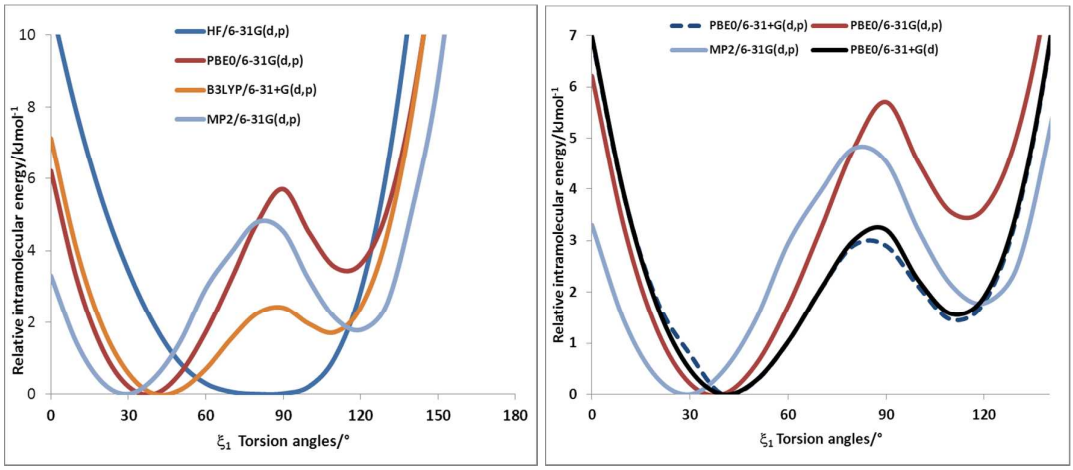

(a) (b)

Figure S3: The relative conformational energy as a function of the ξ_1 torsion angle of isolated tolfenamic acid calculated at different levels of theory. (a) The effect of different methods (b) The effect of increasing the basis set with the PBE0 hybrid functional.

3.2. Consideration of ξ_2 torsion angle

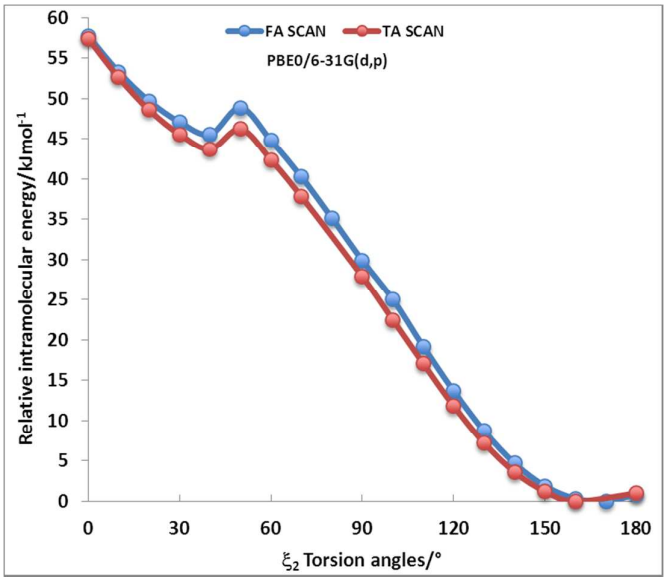

Figure S4: The relative conformational energy as a function of the ξ_2 torsion angle of FA and TA calculated at PBE0/6-31G(d,p) level of theory. 180° is as depicted in Figure S5.

Conformational energy scan of ξ_2 (Figure S4) of TA and PBA are very similar. As the torsion angle decreases from 180°, the intramolecular hydrogen bond between the carbonyl group and N-H becomes strained and eventually breaks hence the huge energy penalty observed for any major change in torsion angle. Therefore the ξ_2 torsion could be kept rigid during the search, but was optimized within the crystal structures in step 3.

3.3. Further details on Crystal Energy Landscape calculations and intermediate results

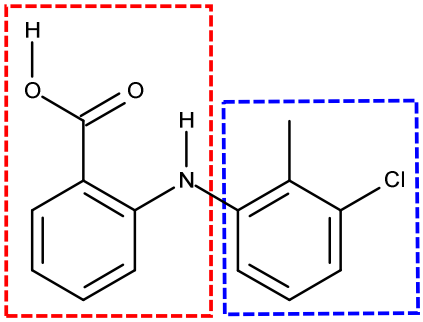

Figure S5: Fragment used for CrystalPredictor search for TA. Each fragment was kept rigid during the search for hypothetical crystal structures.

CrystalPredictor (**step 1**) searches were carried out on TA and FA with two separate fragments (Figure S5) kept rigid, while the ξ_1 torsion (Figure S1c) was treated as a flexible torsion. The lattice energy was then crudely calculated by minimizing the sum of the intermolecular (estimated from the Williams potential for the repulsion-dispersion contribution and interpolated, variable ESP charges for the electrostatics contribution) and intramolecular contributions (interpolated from the intramolecular grid). 250,000 lattice energy minimizations were executed. This resulted in 162,288 and 182,615 distinct structures, 16,543 and 22,884 of which were unique for TA (Figure S6a) and FA respectively.

The lattice energy calculation was refined in steps, increasing the computational cost but decreasing the number of structures been examined as our confidence in the ranking increased. After single point calculations on all of the unique crystal structures (**step 2**), the gap between the known form and the global minima reduces from 40 $kJmol^{-1}$ to 6 $kJmol^{-1}$ (Figure S6).

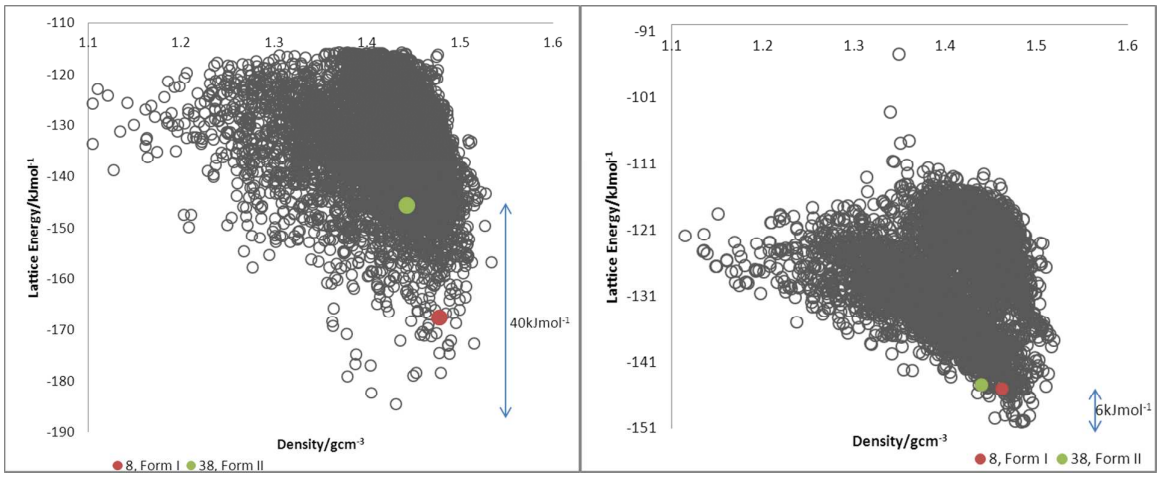

(a) (b)

Figure S6: Crystal energy landscape of TA for Z'=1 structure after (a) CrystalPredictor (**Step 1**) **(b)** single conformer calculation of ΔE_{intra} and the atomic multipoles at PBE0/6-31G(d,p) level of theory, and rigid molecule crystal structure optimization (**Step 2**)

The crystal energy landscape after CrystalOptimizer calculations on 100 of the most stable crystal structures at PBE0/6-31+G(d) level of theory, **Step 3**, were compared with the PCM calculations, **step 4** (Figure S7). The introduction of the dielectric continuum (Figure S7) reorders some of the nearly equi-energetic low energy crystal structures. For example, two of the most stable forms of TA, form I and II, switched their relative rank when a dielectric continuum was introduced and there was also a noticeable increase in stability of the Z=2 crystal structure models of TA form V (Figure S7 bottom). The experimental and global minimum structures on the crystal energy landscape of FA become closer in energy and density (Figure S7 top).

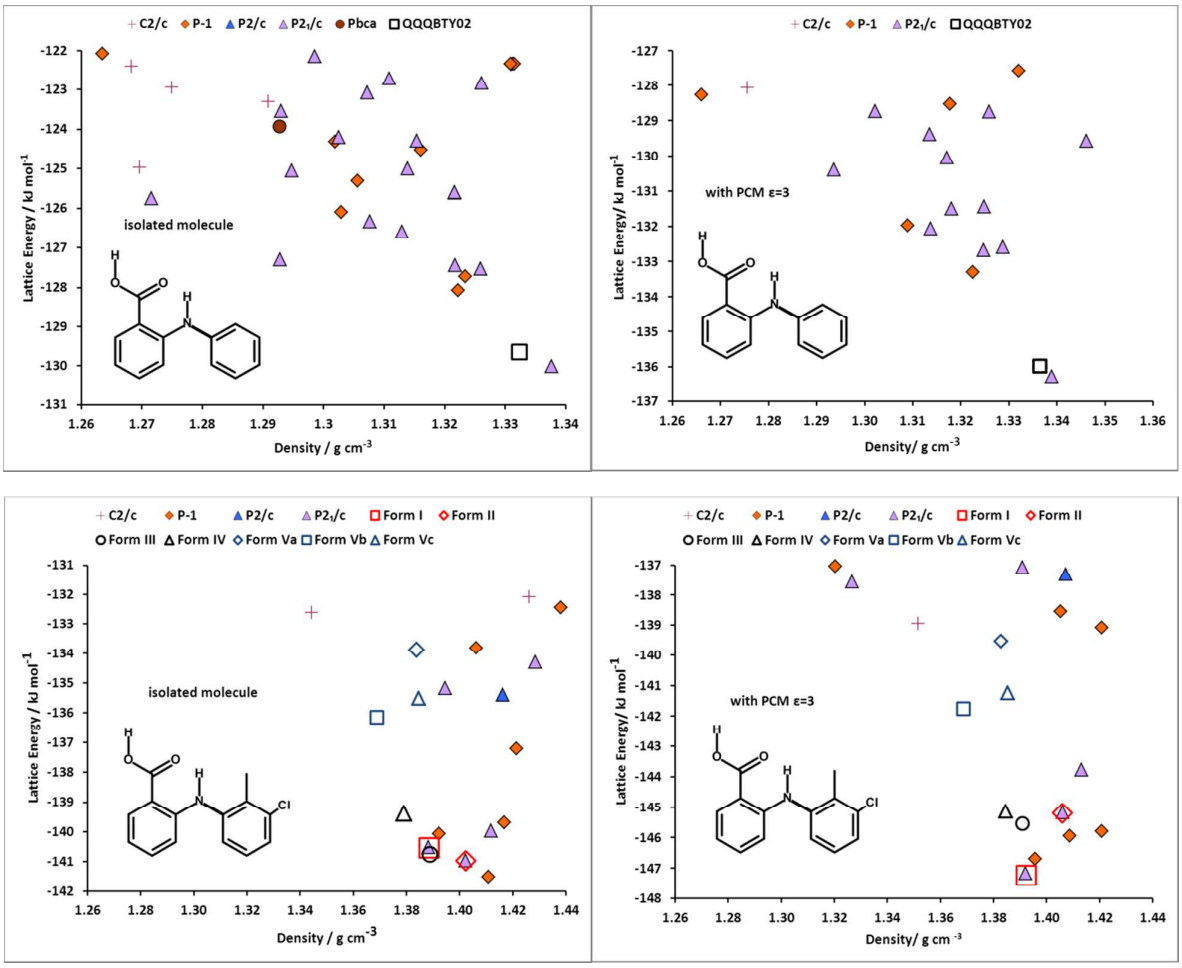

Figure S7: Crystal energy landscapes for (top) FA and (bottom) TA after CrystalOptimizer (left) and PCM calculations (right) (**step 3 and 4**). Solid symbols are structures generated in the search, with open symbols denoting the lattice energy minima for the known structures.

3.4. The structures of the final crystal energy landscapes.

All structures in Table 1 and 2 are available in shelx (.res) format from the authors.

Table S1: Fenamic acid lattice energy minima shown on Figure 7. The minimum found starting from the experimental structure is in bold.

Label	SG	a Å	b Å	c Å	α °	β °	γ °	ρ gcm^{-3}	U_{inter} $kJmol^{-1}$	ΔE_{intra} $kJmol^{-1}$	E_{latt} $kJmol^{-1}$
#1FA_22	*$P2_1/c$*	8.68	4.68	27.09	90.00	74.04	90.00	1.34	-137.65	1.37	-136.28
QQQBTY02	***P-1***	**8.48**	**9.91**	**13.33**	**90.94**	**88.16**	**71.30**	**1.34**	**-139.2**	**3.16**	**-135.99**
#2FA_2	*P-1*	4.54	9.27	14.93	69.10	92.01	68.58	1.32	-134.83	1.52	-133.31
#3FA_59	*$P2_1/c$*	4.57	8.80	26.95	90.00	99.56	90.00	1.32	-133.81	1.13	-132.69
#4FA_1	*$P2_1/c$*	4.51	8.99	26.82	90.00	78.77	90.00	1.33	-134.35	1.75	-132.60
#5FA_10	*$P2_1/c$*	4.58	26.86	8.80	90.00	85.26	90.00	1.31	-133.50	1.44	-132.06
#6FA_151	*P-1*	12.85	7.44	6.66	66.29	102.74	111.27	1.31	-134.18	2.21	-131.97
#7FA_4	*$P2_1/c$*	17.88	5.34	12.83	90.00	61.36	90.00	1.32	-145.12	13.63	-131.49
#8FA_16	*$P2_1/n$*	13.95	5.20	15.08	90.00	78.09	90.00	1.32	-145.05	13.61	-131.44
#9FA_287	*$P2_1/n$*	14.29	4.59	17.70	90.00	70.60	90.00	1.29	-132.79	2.40	-130.39
#10FA_192	*$P2_1/c$*	4.60	19.18	12.31	90.00	97.92	90.00	1.32	-136.41	6.36	-130.05
#11FA_19	*$P2_1/c$*	5.01	21.79	10.04	90.00	73.77	90.00	1.35	-143.77	14.19	-129.58
#12FA_23	*$P2_1/c$*	6.44	34.25	6.53	90.00	131.52	90.00	1.31	-138.55	9.17	-129.38
#13FA_2880	*$P2_1/n$*	14.90	4.93	14.56	90.00	88.25	90.00	1.33	-136.66	7.91	-128.75
#14FA_33	*$P2_1/c$*	4.30	26.00	9.97	90.00	102.50	90.00	1.30	-130.39	1.66	-128.73
#15FA_18	*P-1*	8.70	7.99	9.35	105.83	102.20	113.01	1.32	-130.40	1.87	-128.53
#16FA_5226	*P-1*	10.21	13.25	9.90	141.09	116.96	43.47	1.27	-130.13	1.86	-128.27
#17FA_484	*C2/c*	38.64	8.97	7.50	90.00	58.74	90.00	1.28	-129.62	1.55	-128.07
#18FA_7	*P-1*	4.99	11.13	9.95	84.46	104.67	92.66	1.33	-141.67	14.09	-127.58

Table S2: Tolfenamic acid lattice energy minima shown on Figure 7. Minima found starting from the experimental structures, or ordered models, are in bold.

Label	SG	a Å	b Å	c Å	α °	β °	γ °	ρ gcm^{-3}	U_{inter} $kJmol^{-1}$	ΔE_{intra} $kJmol^{-1}$	E_{latt} $kJmol^{-1}$
FORM I	***P2$_1$/c***	**4.86**	**31.54**	**8.32**	**90.00**	**102.00**	**90.00**	**1.39**	**-148.74**	**1.50**	**-147.24**
#1TA_8	*P2$_1$/c*	4.85	31.60	8.33	90.00	77.87	90.00	1.39	-148.65	1.48	-147.17
#2TA_15	*P-1*	17.72	8.47	4.84	79.49	112.37	111.71	1.40	-148.32	1.63	-146.69
#3TA_876	*P-1*	16.98	7.44	7.34	94.40	93.76	41.81	1.41	-149.52	3.57	-145.95
#4TA_6243	*P-1*	12.06	10.15	8.71	71.76	61.70	117.37	1.42	-147.74	1.96	-145.79
FORM III	***P2$_1$/c***	**7.83**	**11.64**	**27.48**	**90.00**	**93.32**	**90.00**	**1.39**	**-148.53**	**2.98**	**-145.55**
FORM II	***P2$_1$/n***	**3.86**	**22.06**	**14.60**	**90.00**	**96.21**	**90.00**	**1.41**	**-147.84**	**2.63**	**-145.21**
#5TA_38	*P2$_1$/n*	3.86	22.05	14.60	90.00	83.76	90.00	1.41	-147.81	2.63	-145.18
FORM IV	***P-1***	**7.65**	**14.00**	**18.28**	**102.56**	**99.32**	**91.52**	**1.38**	**-147.73**	**2.59**	**-145.14**
#6TA_82	*P2$_1$/c*	3.90	14.33	23.74	90.00	68.05	90.00	1.41	-146.11	2.34	-143.77
FORM V_b	***P-1***	**6.78**	**10.77**	**8.97**	**92.75**	**85.03**	**103.48**	**1.37**	**-145.05**	**3.28**	**-141.77**
FORM V_c	***P-1***	**7.68**	**9.28**	**9.49**	**106.95**	**92.51**	**102.49**	**1.39**	**-144.37**	**3.13**	**-141.24**
FORM V_a	***P-1***	**7.67**	**9.19**	**9.61**	**107.56**	**93.99**	**100.87**	**1.38**	**-142.19**	**2.65**	**-139.54**
#7TA_45	*P-1*	14.44	12.31	3.85	109.50	83.30	76.31	1.42	-141.71	2.63	-139.08
#8TA_88	*C2/c*	26.97	4.79	20.67	90.00	105.67	90.00	1.35	-141.13	2.18	-138.95
#9TA_64	*P-1*	7.56	9.00	9.86	75.31	101.45	80.29	1.41	-147.44	8.89	-138.55
#10TA_153	*P2$_1$/c*	4.92	12.39	22.17	90.00	75.74	90.00	1.33	-139.51	1.96	-137.55
#11TA_80	*P2/n*	14.92	3.98	21.50	90.00	75.36	90.00	1.41	-139.10	1.80	-137.30
#12TA_3630	*P2$_1$/c*	16.55	3.84	23.38	90.00	57.14	90.00	1.39	-139.30	2.22	-137.08

4. Further comparisons of the hypothetical structures of FA on the crystal energy landscape and known form of TA

The hypothetical crystal structures on the crystal energy landscape of FA (Figure S8) are similar to some of the known forms of TA (forms I-IV), with some of these hypothetical crystal structures overlaying up to 13 molecules (forms I and III of TA, Figure S8). Many of the low energy structures of FA have more in common with a polymorph of TA than the only known form of FA i.e. the second numbers are greater than the first bold numbers (Figure S8), with a few exceptions. There are distinct crystal structures of FA with the molecule planar (highlighted in Figure S8).

The similarities between the known form of TA and the hypothetically generated structures of FA confirm that the effect of the substituents CH_3 and Cl on the relative energies cause the energy landscape of TA to be more polymorphic than FA (Figure S7).

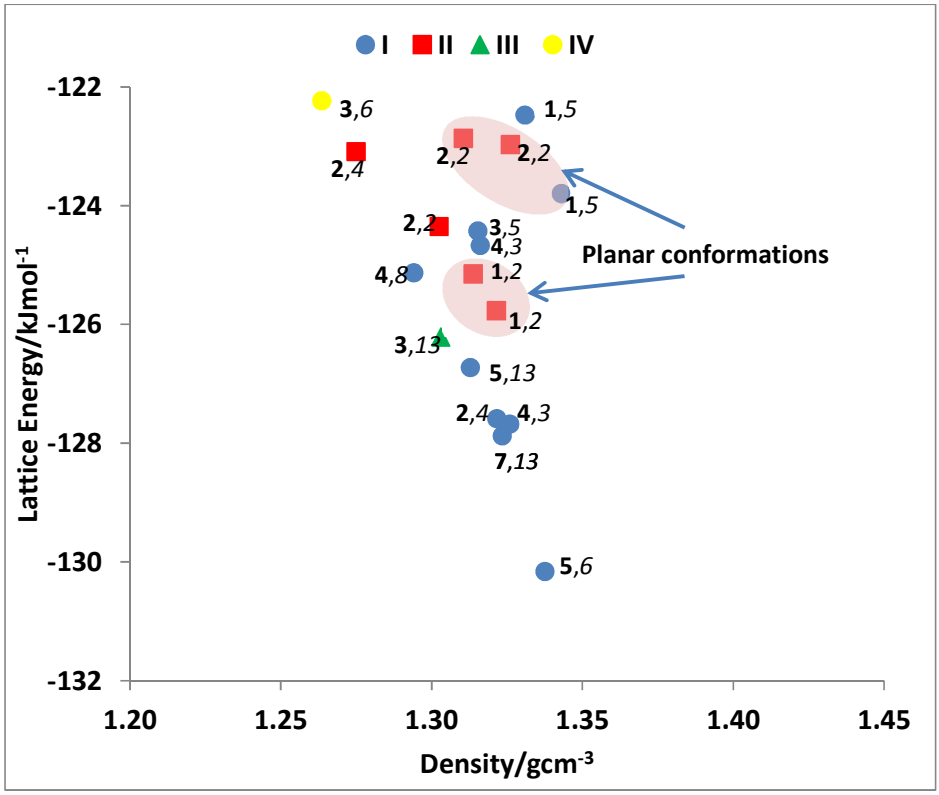

Figure S8: Classification of the crystal energy landscapes of FA in terms of the similarity of the structures to those of known TA polymorphs (I-IV). Each point is colored by the TA polymorph with which it overlay the greatest number *n* of molecules, in a Crystal Packing Similarity calculation which ignores the CH_3 and Cl. Numbers in **bold** give the number of molecules which overlay with the known structure of FA. Hence a label **5**,*6* on a structure represented by a blue circle means the structure overlays **5** molecules with the experimental form of FA but *6* with form I of TA.

5. Comparison with the newly published crystal structures of flufenamic acid

Table S3: Crystal Packing Similarity comparisons of the newly published structures of flufenamic acid[7] and the experimental structures of FA and TA (with 3 ordered models for form V) and their most stable hypothetical crystal structures (extension of Table 5). The similarity is given in the form n(RMSD$_n$), with the overlays of four or more molecules highlighted.

	n(**RMSD$_n$/Å**)					
	FPAMCA_2	FPAMCA_4	FPAMCA_5	FPAMCA_6	FPAMCA_7	FPAMCA_8
FA						
QQQBTY02	**5(1.49)**	3(0.79)	2(0.73)	**4(1.60)**	2(0.43)	3(0.82)
#1FA_22	**4(1.62)**	**5(1.42)**	2(1.05)	**5(2.02)**	2(0.22)	2(0.26)
#2FA_2	**4(1.51)**	**4(0.34)**	3(1.19)	**5(0.80)**	2(0.21)	3(1.30)
TA						
II	2(0.10)	2(0.16)	2(0.4)	2(0.17)	1(0.71)	2(0.81)
I	3(1.58)	2(0.54)	2(0.69)	4(2.10)	2(0.34)	2(0.41)
III	2(0.22)	2(0.24)	**4(0.52)**	2(0.25)	1(0.64)	2(0.77)
IV	2(0.20)	2(0.23)	**4(1.68)**	3(0.84)	2(0.64)	2(0.70)
V_a	3(1.24)	2(0.48)	2(0.64)	2(0.50)	3(0.68)	3(0.80)
V_b	**5(0.54)**	3(0.67)	2(0.45)	3(0.63)	1(0.59)	2(0.78)
V_c	2(0.85)	2(0.41)	2(0.79)	2(0.42)	2(0.77)	3(1.27)
#2TA_15	**4(3.04)**	2(0.80)	2(0.17)	2(0.62)	3(0.42)	**4(2.80)**
#3TA_876	**4(1.34)**	2(0.18)	**4(2.10)**	2(0.19)	1(0.76)	2(0.82)
#4TA_6243	**4(1.10)**	2(0.58)	2(0.40)	2(0.60)	2(0.31)	2(0.38)
#6TA_82	2(0.18)	2(0.19)	2(0.25)	2(0.20)	1(0.73)	2(0.81)

Reference List

1. Surov, A. O.; Szterner, P.; Zielenkiewicz, W.; Perlovich, G. L. Thermodynamic and structural study of tolfenamic acid polymorphs *J. Pharm. Biomed. Anal.* **2009,** *50*, 831-840.

2. Brittain, H. G. *Polymorphism in Pharmaceutical Solids;* Brittain, H. G., Ed. Informa Healthcare: New York, London, 2009; Vol. 192.

3. Mattei, A.; Li, T. Polymorph Formation and Nucleation Mechanism of Tolfenamic Acid in Solution: An Investigation of Pre-nucleation Solute Association *Pharmaceut. Res.* **2012,** *29*, 460-470.

4. Andersen, K. V.; Larsen, S.; Alhede, B.; Gelting, N.; Buchardt, O. Characterization of two polymorphic forms of tolfenamic acid, N-(2-methyl-3-chlorophenyl)anthranilic acid: their crystal structures and relative stabilities *J. Chem. Soc. Perkin Trans 2* **1989,** 1443-1447.

5. Lopez-Mejias, V.; Kampf, J. W.; Matzger, A. J. Polymer-Induced Heteronucleation of Tolfenamic Acid: Structural Investigation of a Pentamorph *J. Am. Chem. Soc.* **2009,** *131*, 4554-4555.

6. *Gaussian 03,* Frisch, M. J. et al. Gaussian Inc.: Wallingford CT, 2004

7. Lopez-Mejias, V.; Kampf, J. W.; Matzger, A. J. Nonamorphism in Flufenamic Acid and a New Record for a Polymorphic Compound with Solved Structures *J. Am. Chem. Soc.* **2012,** *134*, 9872-9875.